

## PUBLISHER'S NOTE

# Publisher's Note: Temporally distinct roles of ATM and ROS in genotoxic-stress-dependent induction and maintenance of cellular senescence

Raji R. Nair, Meisam Bagheri and Deepak Kumar Saini

There is an error in *J. Cell Sci.* (2015) 128, 342-353 (doi:10.1242/jcs.159517).

An issue with cell images in Fig. 1C (BrdU treated) and Fig. 2B (100  $\mu$ M) was raised on PubPeer. These two panels show the same field of cells but in different orientations. The authors state that these cells were selected as results show the same experimental conditions (100  $\mu$ M BrdU treatment) and they chose to highlight a different cell in each case.

An alternative cell for these conditions is shown in the new Fig. 2B here.

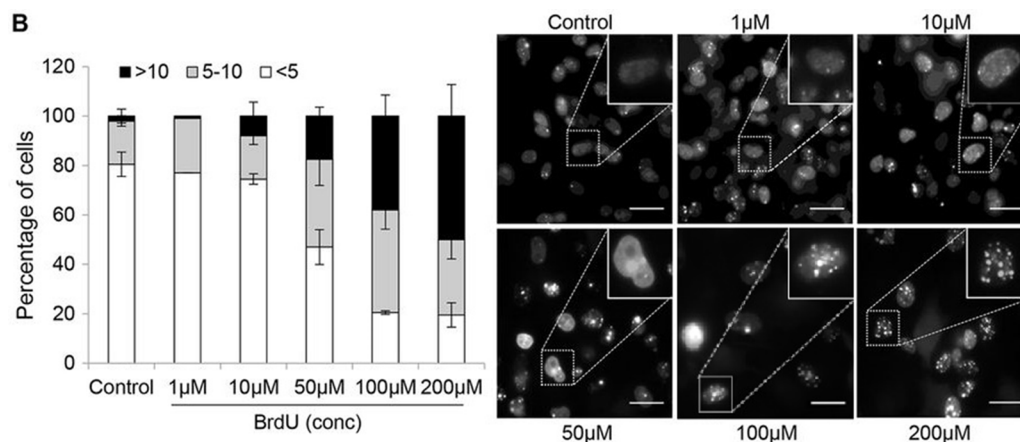


**Fig. 2B. Activation of the DDR pathway is directly proportional to the amount of DNA damage.** For all experiments, HeLa cells were treated with the indicated dose of BrdU for 48 to 96 h and analyzed. (B) 53BP foci formation assay. HeLa cells expressing 53BP1-GFP were imaged after 48 h of treatment as described in Fig. 1C. For quantification, the number of punctae present in each cell were counted and the cells were grouped into three categories, less than 5 foci, 5–10 foci and more than 10 foci per cell. On average 100 cells from each experiment were counted ( $n=3$ ). Scale bars: 40  $\mu$ m.

The journal is publishing this note to alert readers to the duplication, which does not impact the conclusions of the paper. The authors apologise for any inconvenience caused.

## RESEARCH ARTICLE

# Temporally distinct roles of ATM and ROS in genotoxic-stress-dependent induction and maintenance of cellular senescence

Raji R. Nair, Meisam Bagheri and Deepak Kumar Saini\*

## ABSTRACT

Cells exposed to genotoxic stress induce cellular senescence through a DNA damage response (DDR) pathway regulated by ATM kinase and reactive oxygen species (ROS). Here, we show that the regulatory roles for ATM kinase and ROS differ during induction and maintenance of cellular senescence. Cells treated with different genotoxic agents were analyzed using specific pathway markers and inhibitors to determine that ATM kinase activation is directly proportional to the dose of the genotoxic stress and that senescence initiation is not dependent on ROS or the p53 status of cells. Cells in which ROS was quenched still activated ATM and initiated the DDR when insulted, and progressed normally to senescence. By contrast, maintenance of a viable senescent state required the presence of ROS as well as activated ATM. Inhibition or removal of either of the components caused cell death in senescent cells, through a deregulated ATM–ROS axis. Overall, our work demonstrates existence of an intricate temporal hierarchy between genotoxic stress, DDR and ROS in cellular senescence. Our model reports the existence of different stages of cellular senescence with distinct regulatory networks.

**KEY WORDS:** Cellular senescence, DNA damage response, Reactive oxygen species, ATM kinase

## INTRODUCTION

Cellular senescence is an irreversible state of cell cycle arrest, during which the cells do not divide, yet remain viable. Various studies, some of which were done way back in 1965 (Hayflick, 1965), have proposed that cellular senescence is equivalent to organismal aging (Chen et al., 2007; Jeyapalan and Sedivy, 2008; Schneider and Mitsui, 1976). In addition, many recent studies show that cellular senescence is one of the outcomes of the cell fate decision process, where a cell halts the cell cycle if the accumulated genomic errors cannot be repaired, and it would be detrimental if such errors were left unrepaired. In a normal cell, the accumulation of DNA damage can also trigger activation of oncogenes or deactivation of tumor suppressor genes, which can initiate carcinogenesis or cell death response might be initiated, though only the latter can be true for cancer cells (Surova and Zhivotovsky, 2013). Given that both outcomes, death and carcinogenesis, are harmful, to maintain cellular viability the senescence growth arrest program can also be initiated through a cell fate decision process that is not very well characterized. This

pro-survival choice makes cellular senescence a protective process, where cell viability is maintained in face of the deleterious effects of accumulated DNA damage that could either lead to cell death or formation of cancers if left unchecked. However, as the organism gets older, there is a concomitant increase in number of these damaged and senescent cells, which leads to the accumulation of pro-inflammatory and pro-proliferative molecules, which are secreted by these cells, thereby generating a prime niche for cancer formation and making senescence a harmful process. The net summation of these outcomes makes senescence antagonistically pleiotropic, where it is protective in a cell autonomous manner and deleterious in non-autonomous manner (Coppé et al., 2010; Freund et al., 2010; Itahana et al., 2007).

The existing evidence suggests that the senescence condition of cells depends on their ability to maintain a persistent DNA damage state without inducing death or repair (d'Adda di Fagagna, 2008). This assumption is also supported through a number of models used for inducing cellular senescence in cultured cells. The models include: replicative exhaustion of primary mortal cell lines, which causes replicative senescence (Aliouat-Denis et al., 2005; Hayflick, 1965); exposure of cells to genotoxic stress such as  $\gamma$  rays,  $H_2O_2$  etc, causing stress-induced senescence (Chen and Ames, 1994; Duan et al., 2005); and by hyperactivating oncogenes in cells, which causes oncogene-induced senescence (Serrano et al., 1997). Whereas genotoxic stress leads to direct DNA damage, in oncogene activation and replicative exhaustion the DNA damage occurs through accumulation of errors during DNA replication and telomere shortening during every cell division (Chen et al., 2007; Di Micco et al., 2006; Maicher et al., 2012). Increasing evidence has implicated a number of molecules as being crucial for regulating cell fates after DNA damage, which includes ATM kinase, p53 and reactive oxygen species (ROS). It has been shown that genotoxic agents such as  $\gamma$  rays,  $H_2O_2$  etc generate ROS inside the cells, causing DNA damage (Cooke et al., 2003; Mishra, 2004), which triggers the DNA damage response (DDR), followed by senescence. This suggests that there is an integral role for ROS in the cellular senescence program and, consistent with this idea, elevated ROS levels have also been reported in cells in which senescence has been induced by replicative exhaustion or by oncogene activation (Colavitti and Finkel, 2005; Lee et al., 1999).

In the present study, we show that direct DNA damage activates the DDR and induces cellular senescence through an ATM-kinase-mediated pathway that is independent of ROS. However, both ATM kinase and ROS were found to be crucial for maintenance of senescence. Our findings hence show that senescence can be divided into two temporally distinct stages, initiation or early senescence, and the maintenance stage of senescence. Our findings about the roles played by ATM and ROS help explain many

Department of Molecular Reproduction, Development and Genetics, Indian Institute of Science, Bangalore 560012, India.

\*Author for correspondence (deepak@mrdg.iisc.ernet.in)

Received 14 July 2014; Accepted 18 November 2014

previous reports where disparate observations have been made because such discrepancies could be due to differences in the senescence stage in which the experiments were performed and the methods which were used for senescence generation (Barascu et al., 2012; Lee et al., 1999; Passos and Von Zglinicki, 2006; Pospelova et al., 2009; Qu et al., 2014). Overall, the presence of temporally linked ROS-dependent and -independent events in cellular senescence are described, which are mediated by ATM kinase and are independent of p53 protein.

## RESULTS

### ATM activation and ROS induction in cells exposed to genotoxic stress

Our initial experiment was performed to evaluate the activation of ATM kinase and ROS generation in cells exposed to genotoxic stress in order to identify whether they play a role in stress-mediated cellular senescence. For this, HeLa cells were treated with 0.1  $\mu\text{M}$  doxorubicin (Dox) or 100  $\mu\text{M}$  of 5-bromodeoxyuridine (BrdU), a thymidine analog, which are genotoxic stress agents with different modes of action. Whereas BrdU gets incorporated in the DNA and causes DNA damage, Dox affects cells on many levels and its actions are very diverse (Gewirtz, 1999; Thorn et al., 2011). Although some studies show that cytotoxic effects of Dox are mediated through its inhibitory effect on DNA topoisomerase (Tewey et al., 1984), others suggest that it induces generation of toxic free radicals (Mizutani et al., 2005; Mukhopadhyay et al., 2009) or that the mechanism of its action is still not clear (Sliwiska et al., 2009). Substantial levels of proliferation arrest and activation of ATM kinase were detected in cells exposed to BrdU after 48 h,

as monitored by the presence of phosphorylation of the histone H2AX protein ( $\gamma\text{H2AX}$ ), a substrate of ATM kinase (Fig. 1A). Surprisingly, the cells exposed to Dox did not show H2AX phosphorylation at 48 h (Fig. 1A, lane 3), but the presence of the DDR in Dox-treated cells was confirmed using an alternative DDR assay (described below).

After confirming the activation of ATM kinase by genotoxic stress, the presence of ROS in the treated cells was then evaluated using a reporter dye, 2',7'-dichlorofluorescein diacetate (DCFDA), which becomes fluorescent in presence of ROS. In BrdU- and Dox-treated cells, elevated ROS levels were detected (Fig. 1B), similar to what has been reported previously (Kang et al., 2012). In Dox-treated cells, more cell death was recorded compared to those treated with BrdU, indicating the presence of higher levels of stress; however, in both the treatments, proliferation was arrested and cells entered a senescent-like state (see later). These initial experiments confirmed that genotoxic stress activates both ATM kinase and ROS production, which can lead to growth arrest.

### Direct DNA damage activates the DDR and ATM kinase

As observed previously and successfully reproduced in our preliminary experiments, Dox can induce cell cycle arrest by preventing DNA unwinding by inhibiting DNA topoisomerase II (Tewey et al., 1984), which affects both replication and transcription (van Maanen et al., 1988; Yokochi and Robertson, 2004). The same outcome can be obtained when cells are exposed to ionizing radiation, which activates multiple cellular stress pathways, including the DDR pathway (Gewirtz, 1999; Kanaar

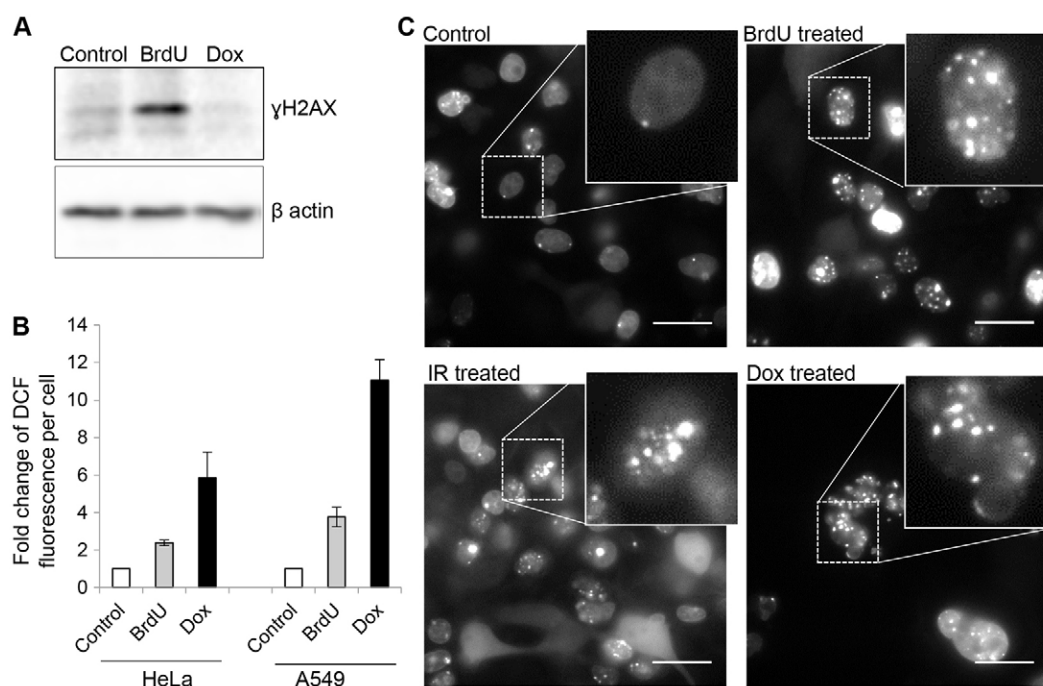


**Fig. 1. Effect of genotoxic stress on activation of DNA damage response.** (A)  $\gamma\text{H2AX}$  analysis. Total protein from control untreated cells and HeLa cells treated for 48 h with 100  $\mu\text{M}$  BrdU and 0.1  $\mu\text{M}$  doxorubicin was used for western blotting. The blot was probed with anti-phospho-H2AX and anti- $\beta$ -actin antibodies followed by HRP-conjugated anti-rabbit-IgG secondary antibody. A representative blot from three experiments is shown. (B) ROS quantification. HeLa and A549 cells, were seeded at a density of 10,000 cells per well in a 24-well plate. Cells were treated with 100  $\mu\text{M}$  BrdU or 0.1  $\mu\text{M}$  doxorubicin for 48 h. ROS levels were estimated as described in the Materials and Methods. Levels are normalized those in control cells set at 1 (mean  $\pm$  s.e.m.;  $n=5$ ). (C) 53BP foci formation assay. HeLa cells, stably expressing GFP-53BP1 fusion protein were used and treated with 100  $\mu\text{M}$  BrdU, 1 Gy ionizing radiation radiation or 0.1  $\mu\text{M}$  Doxorubicin for 48 h. The cells were imaged for GFP distribution as described in Materials and Methods. A representative image from three experiments is shown. Inset, magnified image of one of the cells showing foci. Scale bars: 40  $\mu\text{m}$ .

et al., 1998). Given that multiple signaling pathways are triggered by Dox and ionizing radiation, including those which can lead to direct DNA damage, we decided to utilize BrdU as an agent for activating the DDR (Erol, 2011) and inducing senescence for all our subsequent studies. This was essential because both Dox and ionizing radiation are highly toxic (Thorn et al., 2011) and extremely high levels of ROS were detected upon Dox treatment (Fig. 1B), which might be responsible for its DNA-damaging effect (Mizutani et al., 2005; van Maanen et al., 1988), thereby limiting their use in our experiments (because they would not permit ROS-independent analysis of senescence). BrdU, previously explored as an anti-cancer drug, has recently been shown to induce cellular senescence in proliferating HeLa cells, similar to that which occurs in replicatively senescent cells (Suzuki et al., 2001). It is expected that being a nucleotide analog, it will be directly incorporated into the DNA, thereby affecting replication and leading to cell cycle arrest. With the experiments described above, it was confirmed that direct DNA damage induced by BrdU can induce the DDR, which might lead to growth arrest and activate pathways leading to cellular senescence.

Given that the primary rationale of using BrdU was that it can induce DNA damage by direct incorporation into the DNA, the presence of DNA double-strand breaks (DSBs) in the treated cells was evaluated by a 53BP1 foci formation assay. GFP-tagged 53BP1 protein (Zgheib et al., 2009) was stably transfected in HeLa cells and its distribution in response to BrdU treatment was examined. Distinct ‘punctate like’ foci of 53BP1–GFP were detected within 24 to 48 h of treatment (Fig. 1C), suggesting that BrdU activates the DDR through introducing DSBs, which then activates ATM kinase and recruits 53BP1–GFP to the site of damage. To confirm that foci detected are indeed DSBs, the presence of foci were evaluated in cells treated with Dox or with 1 Gy ionizing radiation, which is known to cause DSBs. Distinct 53BP1 foci after these treatments were also observed (Fig. 1C, lower panels), thereby confirming that genotoxic effect of BrdU is through formation of DSBs, which activate ATM kinase (Ditch and Paull, 2012; Guo et al., 2010; Lee and Paull, 2005). Although induction of the DDR by BrdU was slower, as it took 24–48 h for 53BP1 foci to be apparent (supplementary material Fig. S1A), Dox caused more damage and caused foci formation within 8 h post treatment (supplementary material Fig. S1A). These findings strengthen the rationale of using BrdU for all subsequent experiments, as it has a more-specific mechanism of action than other agents.

#### **ATM activation and cell fate is governed by the dose of the direct DNA-damaging agent**

To establish that senescence is indeed one of the cell fate decisions in response to direct DNA damage, a dose–response analysis with BrdU was performed. HeLa cells were treated with varying concentrations of BrdU for 48 to 96 h and analyzed for activation of ATM, proliferation differences, and the proportion of living and dead cells, which are indicators of various cell fates. It was found that with increasing doses of BrdU, there was a concomitant increase in ATM activation (Fig. 2A,B), ROS generation (Fig. 2C) and the percentage of dead cells (Fig. 2D). Although cells treated with sub-lethal doses of BrdU (0.1–10  $\mu$ M) showed the least DDR, they also retained proliferation capacity and had minimal cell death; a concentration of 50  $\mu$ M and above triggered robust DDR pathway responses, ROS generation, growth arrest and caused more cell death. Treatment with 100  $\mu$ M of BrdU led to induction of senescence, similar to what has been observed previously (Cho

et al., 2011), and treatment with a dose of 200  $\mu$ M led to extensive cell death (Fig. 2D) accompanied by maximal ROS generation (Fig. 2C). These experiments established that dose of the DNA-damaging agent is directly proportional to degree of DDR pathway activation, the main regulator of various cell fates under stress conditions.

Cell cycle analysis was then performed to determine the stage in which BrdU-treated cells arrested. Treated cells were found to be trapped predominantly in G1 phase (Fig. 2E) and were prevented from entering the S phase due to replication arrest, similar to what has been reported previously (Mao et al., 2012). To confirm that entry into synthesis phase of cell cycle is crucial for BrdU action, we treated cells that had been starved by culturing them in DMEM containing only 0.1% serum with BrdU, and found that senescence induction was not observed, indicating that the quiescent cells are refractory to BrdU incorporation (data not shown).

On the basis of the above findings, we decided to treat cells with 100  $\mu$ M BrdU for all subsequent experiments to study the role of various molecules in cellular senescence. Initially the cells treated with BrdU were validated for their senescent state by evaluating the presence of an array of senescence-associated markers. This was essential because there is no single assay which can establish the senescence phenotype unequivocally (Itahana et al., 2007; Kuilman et al., 2010; Passos et al., 2009).

#### **Cellular senescence is an outcome of direct DNA damage**

To establish that cellular senescence is an outcome of the DDR, both HeLa and A549 cells were treated with 100  $\mu$ M BrdU and evaluated for the presence of markers associated with cellular senescence. Senescence-associated morphological changes were detected within 48 h and treated cells showed flatter, enlarged and granule-rich morphology (Fig. 3A, top panel), similar to the morphology of replicatively senescent cells reported previously (Dumont et al., 2000; Hayflick, 1965; Leontieva and Blagosklonny, 2010). On average, treated cells were three to four times larger than untreated cells (40–100  $\mu$ m versus 10–30  $\mu$ m for control cells). Given that HeLa cells show extremely low or no expression of active p53 protein (Del Nagro et al., 2014; Matlashewski et al., 1986; Mirzayans et al., 2013), the effect of BrdU treatment on A549 cells, which expresses wild-type p53 protein (supplementary material Fig. S1B) was analyzed (Fig. 3A, bottom panel) so that we could evaluate the role of p53 protein in senescence. As anticipated, p53 expression was not detected in HeLa cells, but induction of p53 protein was seen in A549 cells upon BrdU treatment (supplementary material Fig. S1B). We also validated the changes by treating the cells with 0.1  $\mu$ M Dox, which has previously been shown to induce cellular senescence in a variety of cell types, as a positive control (Sliwinska et al., 2009). Dox treatment induced senescence as marked by senescence-associated  $\beta$ -galactosidase (SA- $\beta$ -gal) positivity (supplementary material Fig. S1C). The cells treated with BrdU also showed the characteristic reduction in the rate of proliferation compared to untreated control cells (Fig. 3B), confirming that the large cells left behind after treatment are non-dividing but viable. Given that the cells were significantly larger, they showed a marked increase in the total protein content (supplementary material Fig. S2A), as well as enhanced metabolic activity, as estimated using a resazurin reduction assay (Fig. 3C).

Analysis of the transcriptional changes in treated cells by quantitative (q)PCR confirmed that cells treated with BrdU

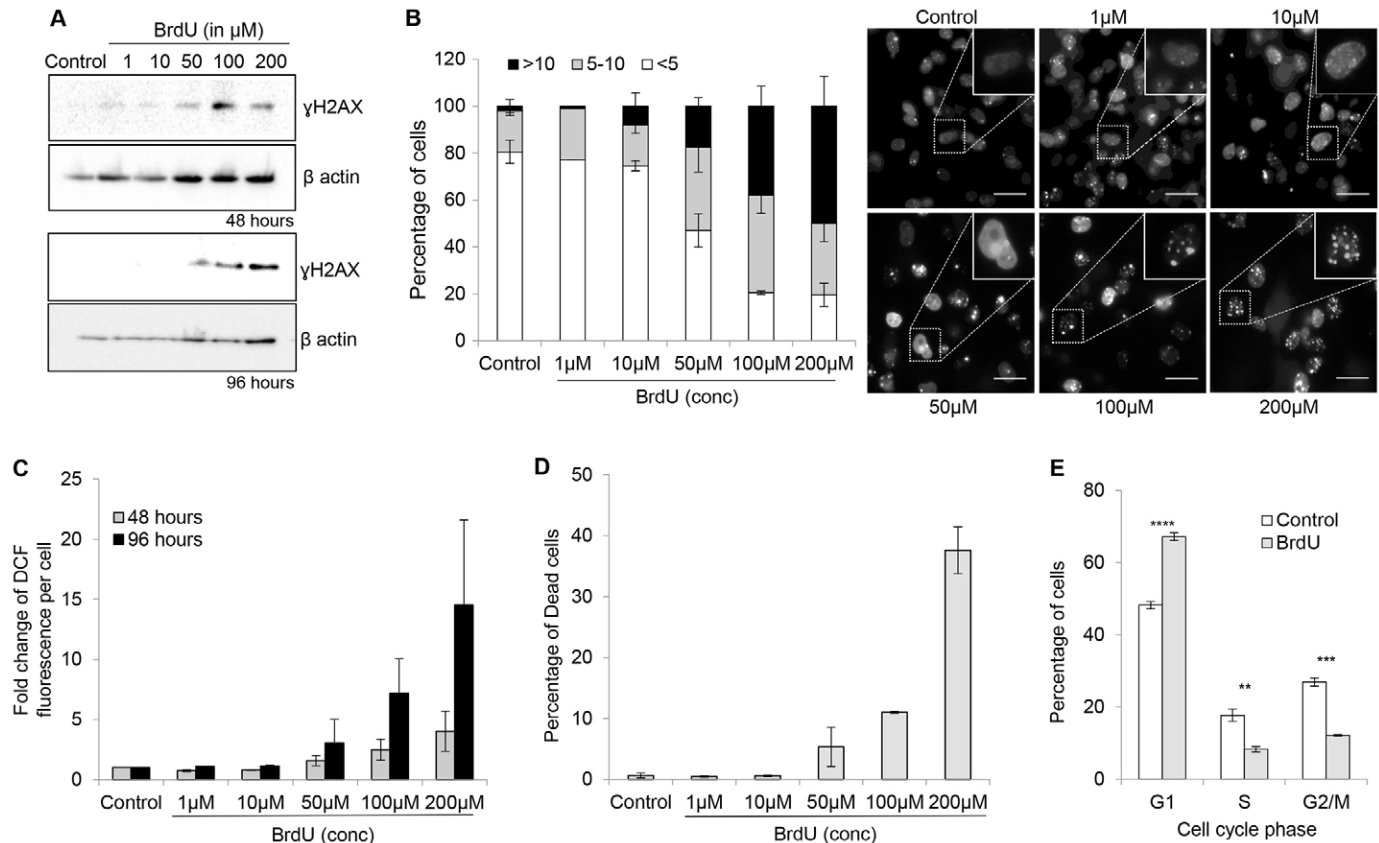


**Fig. 2. Activation of the DDR pathway is directly proportional to the amount of DNA damage.** For all experiments, HeLa cells were treated with the indicated dose of BrdU for 48 to 96 h and analyzed. (A)  $\gamma$ H2AX analysis. Phospho-H2AX and  $\beta$ -actin levels were quantified as described in Fig. 1A. (B) 53BP1 foci formation assay. HeLa cells expressing 53BP1—GFP were imaged after 48 h of treatment as described in Fig. 1C. For quantification, the number of punctae present in each cell were counted and the cells were grouped into three categories, less than 5 foci, 5–10 foci and more than 10 foci per cell. On average 100 cells from each experiment were counted ( $n=3$ ). Scale bars: 40  $\mu$ m. (C) ROS measurements. Treated HeLa cells were used for ROS estimation after 48 or 96 h after treatment as described in Fig. 1B. (D) Dead cell quantification. After 96 h of treatment the floating cells (dead) and adherent cells (live) were collected and counted. The dead cell population is reported as percentage of total cells. (E) Cell cycle analysis. HeLa cells treated with BrdU for 48 h were processed for cell cycle analysis using propidium iodide as described in Material and Methods section and analyzed by flow cytometry ( $n=5$ ). Results are mean  $\pm$  s.e.m. \*\* $P \leq 0.01$ ; \*\*\* $P \leq 0.001$ ; \*\*\*\* $P \leq 0.0001$  (Student's  $t$ -test).

showed enhanced transcription of p21 (also known as CDKN1A), fibronectin,  $\gamma$ 11 and IL8, and a reduction in PCNA (Fig. 3D), all well-established markers for cellular senescence (Coppé et al., 2008; Kumazaki et al., 1991; Lawless et al., 2010; Roninson, 2002). The senescent state of BrdU-treated cells was also confirmed by staining for SA- $\beta$ -gal, the most widely used assay for cellular senescence (supplementary material Fig. S2B) (Dimri et al., 1995). Furthermore, the levels of two pro-inflammatory cytokines, IL6 and IL8, in the secretome of treated cells was also significantly higher compared to untreated cells (Fig. 3E). Next, using conditioned medium from treated cells, the cell-migration-inducing property of the senescence-associated secretory phenotype (SASP) (Krtolica et al., 2001) was tested by performing an *in vitro* wound healing assay. The initial experiments revealed that the secretome was pro-proliferative (supplementary material Fig. S2C); hence, to mask cell proliferation, the wound healing experiments were performed after pre-incubating the injured cells with mitomycin C, which prevents cell proliferation, or with cytochalasin D, which prevents both cell migration and proliferation by inhibiting actin repolymerization. Wound healing was observed in presence of mitomycin C (supplementary material Fig. S2D), whereas no

wound healing was seen when cells were pre-treated with cytochalasin D (supplementary material Fig. S2D), suggesting that SASP of BrdU-induced cells can induce migration (epithelial-to-mesenchymal transition, EMT) as well as proliferation, supporting the hypothesis that cellular senescence has a pro-cancerous effect (Coppé et al., 2010; Krtolica et al., 2001). Overall, using a number of senescence-associated markers, we confirmed that BrdU treatment induces cellular senescence, similar to that which occurs in replicatively senescent cells, at transcriptome, proteome and physiological levels.

#### Direct DNA damage initiates cellular senescence through ATM kinase activation independently of ROS

Once the model was established, we assessed whether ROS and ATM kinase activation was essential for the onset of senescence, using direct DNA damage as a trigger. Previously it has been shown that ROS levels increase during replicative senescence (Furumoto et al., 1998), oncogene-induced senescence (Lee et al., 1999), and in chemical- or stress-induced senescence (Chen and Ames, 1994; Colavitti and Finkel, 2005), similar to what was we observed here (described above in Fig. 1B and Fig. 2C). It is also known that generation of ROS by  $H_2O_2$  exposure is sufficient to

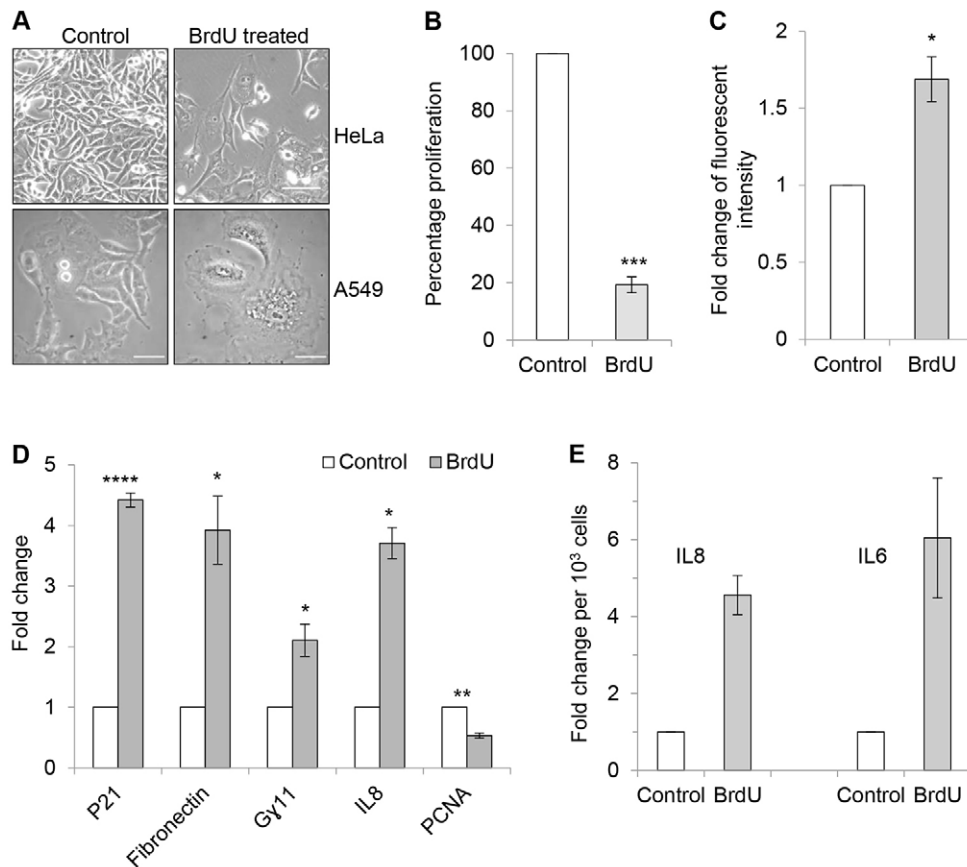


**Fig. 3. Characterization of senescence induced by direct DNA damage.** (A) Morphological changes in cells treated with BrdU. HeLa cells (top panel) and A549 cells (bottom panel) were treated with 100  $\mu$ M BrdU for 48 h and brightfield images were acquired. Left panels, control cells; right panel, BrdU-treated cells. Scale bars: 100  $\mu$ m. (B) Proliferation rate analysis. Cell counting was performed both before and after BrdU treatment and the average cell number in normalized to that in untreated cells (set at 100%) to calculate percentage difference in proliferation with respect to control ( $n=10$ ). (C) Metabolic activity analysis. Equal numbers ( $5 \times 10^3$ ) of normal and senescent cells were seeded per well in a 96-well black plate and a resazurin-based assay was performed as described in the Materials and Methods ( $n=3$ ). The  $y$ -axis represents fold change of fluorescence intensity with respect to untreated cells. (D) Changes in gene expression in BrdU-treated cells. Quantitative RT-PCR analysis to show the change in the expression of p21, fibronectin, G $\gamma$ 11, IL8 and PCNA, in cells treated with BrdU for 48 h with respect to untreated cells. The experiment was performed as described in Materials and Methods. The values were normalized to  $\beta$ -actin expression levels and then control cells to calculate fold changes ( $n>3$ ). (E) Analysis of IL6 and IL8 secretion. HeLa cells were seeded in a 12 well plate at a density of 20,000 cells per well and treated with BrdU for 48 h. The medium from treated and untreated cells was collected and used for sandwich ELISA as per manufacturer's protocol (eBioscience). The cells were counted to obtain cell count and the data are represented as fold change in IL8 or IL6 (pg/ml) secreted per  $10^3$  cells relative to control cells ( $n=5$ ). The conventional representation of secreted amount per  $\mu$ g protein is not used owing to the higher protein content observed in senescent cells (supplementary material Fig. S2A). Results are mean  $\pm$  s.e.m. \* $P \leq 0.05$ ; \*\* $P \leq 0.01$ ; \*\*\* $P \leq 0.001$ ; \*\*\*\* $P \leq 0.0001$  (Student's  $t$ -test).

generate cellular senescence (Chen et al., 2000). We recorded the increase in ROS levels 48 h after induction of direct DNA damage using a plate assay as described above, which was confirmed further in live adherent cells by microscopy (supplementary material Fig. S3A). Interestingly, BrdU-treated cells consistently showed only a marginal increase in the levels of ROS, which was small compared to changes detected in ROS levels in cells treated with Dox (Fig. 1B).

To ascertain the role of ROS, we treated cells with BrdU in the presence of 5 mM N-acetyl L-cysteine (NAC), a ROS quencher (Aruoma et al., 1989; Zafarullah et al., 2003). Although NAC quenched ROS in treated cells (Fig. 4A), the senescence was still activated after 48 h of BrdU treatment, as confirmed by p21 induction (Fig. 4B), SA- $\beta$ -gal positivity (Fig. 4C) and increased IL8 secretion (Fig. 4D). Overall, the senescent cells generated in presence or absence of ROS behaved similarly, indicating that ROS are dispensable during the induction of cellular senescence.

Similar observations were made when p53-positive A549 cells was used in the assays, and although in these cells a significantly higher induction of ROS was observed (Fig. 1B), it was still dispensable for the induction of cellular senescence (supplementary material Fig. S3B,C). This allowed us to speculate that the increase in ROS levels could be due to the high metabolic activity of senescent cells and that it might be an effect of senescence program itself rather than its cause.

Given that ROS was not crucial for senescence induction, we tested whether the DDR was necessary or whether direct incorporation of BrdU was sufficient to halt replication and induce senescence. To block the DDR, ATM kinase activation inhibitors like Ku55933 (Hickson et al., 2004) and caffeine (Blasina et al., 1999), were used during the exposure to DNA-damaging agents. Cells were treated with 10  $\mu$ M Ku55933 or 2 mM caffeine alongside 100  $\mu$ M BrdU for 48 h to induce senescence. The inhibition of ATM activation was confirmed in

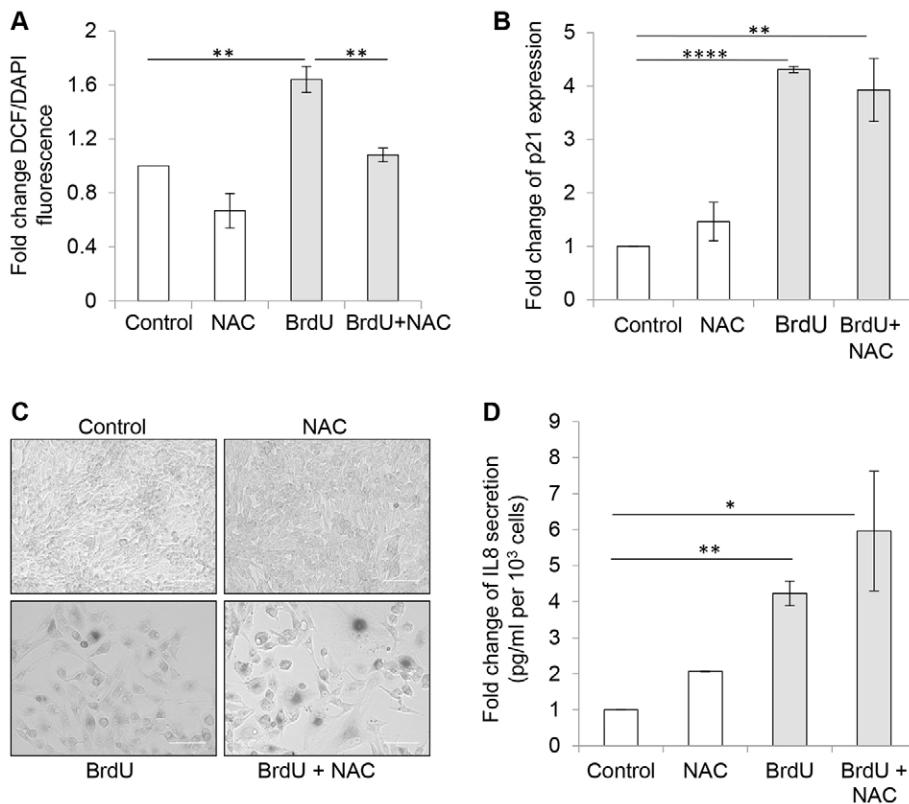


**Fig. 4. Effect of ROS quenching during DNA-damage-induced senescence initiation.**

(A) Effect of NAC on ROS. HeLa cells were treated with 100  $\mu$ M BrdU, 5 mM NAC alone and 5 mM NAC along with 100  $\mu$ M BrdU for 48 h. The levels of ROS were estimated as described in the Materials and Methods as a ratio of FITC:DAPI and normalized to the value in control cells (set at 1). (B) Expression of p21. RT-PCR analysis was performed as described in Fig. 3D to analyze change in the expression of p21 in cells treated with 5 mM NAC along with BrdU. The values were normalized to GAPDH expression and then to the control cells to calculate fold changes ( $n=3$ ). (C) SA- $\beta$ -gal staining of ROS-quenched senescent cells. Cells were treated with 5 mM NAC, BrdU or with NAC+BrdU for 48 h before performing SA- $\beta$ -gal staining and imaging. Images are shown in gray scale. Representative images from three experiments are shown. Scale bars: 100  $\mu$ m. (D) Analysis of IL8 secretion. Cells were treated with 5 mM NAC along with BrdU as described previously. After 48 h, the medium was collected and IL8 ELISA was performed as described in Fig. 3E. Results are mean  $\pm$  s.e.m. \* $P \leq 0.05$ ; \*\* $P \leq 0.01$ ; \*\*\*\* $P \leq 0.0001$  (Student's  $t$ -test).

treated cells by monitoring the reduction in: (1)  $\gamma$ H2AX by using western blotting (Fig. 5A), (2) 53BP1 foci formation by using live-cell imaging (Fig. 5B), and (3) phosphorylated ATM foci by immunofluorescence analysis (Fig. 5C). The treatment with inhibitors prevented cells from entering cellular senescence, as detected by lack of morphological changes and SA- $\beta$ -gal staining (Fig. 5D). To account for the possible non-specific effects of the inhibitors, the role of ATM kinase was also tested by knocking down its expression in HeLa cells using specific short hairpin RNAs (shRNAs) (supplementary material Fig. S4A, inset). The stable knockdown cells where ATM kinase expression was reduced, did not show any growth defect. When these cells were treated with BrdU for 48 h, change in cell fate of knockdown cells was accompanied by activation of cell death in many cells, similar to inhibitor-treated cells. When the ROS levels were evaluated in either inhibitor-treated or knockdown cells, they were found to be elevated, similar to what has been reported previously and as has been observed in ATM-deficient individuals (Ditch and Paull, 2012; Guo et al., 2010; Lee and Paull, 2004; Lee and Paull, 2005), which could explain the observed cell death (Fig. 5E; supplementary material Fig. S4A). These experiments show that although senescence is unconstrained by ROS, ATM kinase activation mediated by the DDR is an absolute requirement for senescence initiation.

#### ATM and ROS are essential for the maintenance of persistent DDR and cellular senescence

Given that the cell fate decision has already been made in senescent cells through ATM activation, we then tested whether the DDR, ATM kinase and ROS play a role in the maintenance of the senescent state in cells. To this end, cells that were in a

senescent state for more than 48 h were tested for both  $\gamma$ H2AX levels (Fig. 6A) and presence of 53BP1 foci (Fig. 6B, top right). The results confirmed that the DDR and ATM kinase were still active in these cells. We then tested whether this persistent DDR, which has been proposed to be crucial for the senescence program (Rodier et al., 2009), is mediated by the presence of the DNA-damaging agent BrdU in the damaged lesions in the cells. Given that it is known that a persistent DDR is triggered when DNA damage cannot be repaired, we replaced the BrdU-containing medium in treated cells with fresh medium after 48 h to record restoration of proliferation by DNA damage repair. However, no proliferation was observed in treated cells, suggesting that growth arrest induced by BrdU is persistent and DNA damage repair pathways are not able to remove incorporated BrdU, thereby maintaining the cells in a viable but senescent state. The presence of BrdU in the washed cells was tested by immunofluorescence microscopy and it was found to be localized as distinct foci, as well as in a diffuse form in the nucleus of the treated cells (supplementary material Fig. S4B), even after 48–72 h of incubation in the fresh medium.

Based on these observations, which confirmed the presence of a persistent DDR, we then evaluated whether activated ATM kinase and ROS were necessary for maintenance of senescence. For this, senescent cells generated by BrdU exposure were treated with the ATM kinase inhibitors caffeine or Ku53393 or the ROS quencher NAC after 48 h, as described in the previous section. As an indicator of ATM kinase inhibition, the presence of 53BP foci was evaluated in these cells, which was found to be significantly lowered when ATM kinase was inhibited (Fig. 6B, bottom right panel), but not in ROS-quenched cells (Fig. 6B, bottom-left panel). However, the treatment with ATM inhibitors induced substantial cell death (Fig. 6C; supplementary material Fig. S4C), perhaps

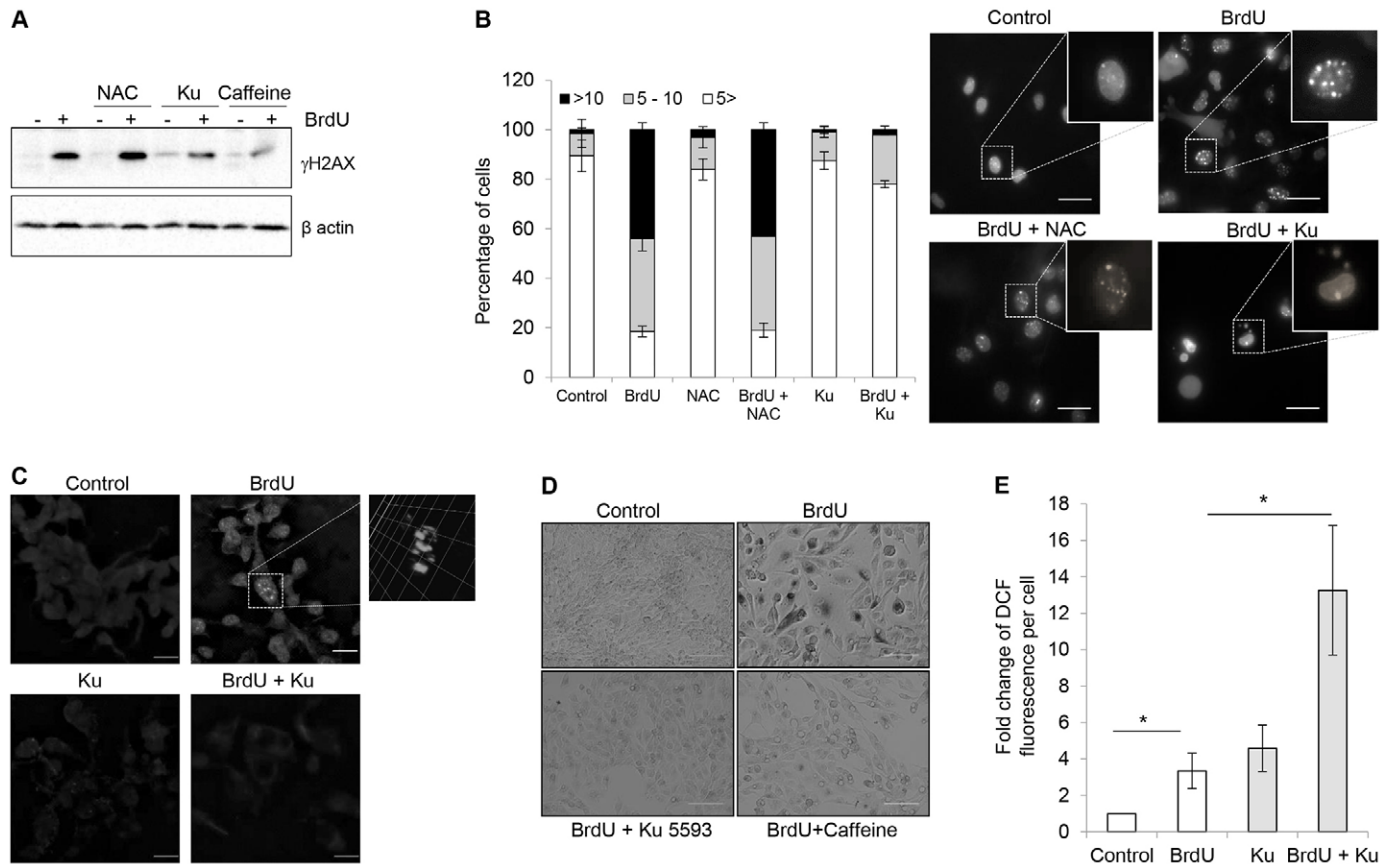


**Fig. 5. Effect of ATM kinase inhibition during DNA-damage-induced senescence initiation.** For all experiments HeLa cells treated with BrdU alone or with 5 mM NAC, 2 mM caffeine or 10  $\mu$ M Ku55933 (Ku) for 48 h were used for (A)  $\gamma$ H2AX analysis. Western blot probed for phospho-H2AX as described in Fig. 1A. A representative blot from two experiments is shown. (B) 53BP1 foci formation assay. HeLa cells stably expressing 53BP1-GFP were treated, imaged and number of foci per cell was recorded as done in Fig. 2B. Scale bars: 40  $\mu$ m. (C) Immunofluorescence analysis for phosphorylated ATM. Cells were processed for phosphorylated ATM staining as described in the Materials and Methods. Anti-phosphorylated-ATM antibody was used at 1:100 dilution followed by anti-rabbit-IgG conjugated to Alexa Fluor 488. The stained cells were mounted with DAPI and imaged as described in the Material and Methods section. A 3D view of the deconvolved image is shown in the upper right image. Representative images from three experiments are shown. Scale bars: 40  $\mu$ m. (D) SA- $\beta$ -gal staining. SA- $\beta$ -gal staining was performed as described in the Material and Methods. Images are shown in gray scale. Representative images from three experiments are shown. Scale bars: 100  $\mu$ m. (E) ROS measurements. HeLa cells were treated with 100  $\mu$ M BrdU, 10  $\mu$ M Ku55933 alone and BrdU along with Ku55933 for 48 h and ROS levels were estimated as described in Fig. 1B. Results are mean  $\pm$  s.e.m. \* $P$   $\leq$  0.05 (Student's *t*-test).

through accumulation of cytotoxic levels of ROS in cells, which was observed in our experiments (Fig. 5E), confirming that ATM kinase acts as an apoptosis inhibitor in senescent cells (Ivanov et al., 2009; Li and Yang, 2010). Interestingly, NAC-treated cells initially maintained their *status quo* (i.e. remained in the senescent state), but later (48 h post-treatment), these cells also died (Fig. 6C), similar to ATM-kinase-inhibited cells. This suggests that the presence of activated ATM-ROS axis is necessary for maintaining the senescent state in the cells. The results suggest that there is a DDR-ROS-ATM signaling loop, which ensures that viability is maintained in senescent cells. In this autoregulatory model, ATM kinase quenches ROS and prevents associated cell death. At the same time elevated ROS levels in senescent cells keep ATM kinase in activated state thereby maintaining the senescent status of the cells (Fig. 7).

#### p53 is not essential for inducing cellular senescence

Finally, by virtue of utilizing various cell lines which inherently have differences in p53 expression, we evaluated the role of p53 protein in initiation and maintenance of cellular senescence. In

our studies, we have reported findings using A549 cells, which is a lung epithelial cell line harboring wild-type p53 protein, and HeLa cells, a cervical carcinoma cell line which is p53 negative by virtue of expression of HCV E6 antigen which degrades p53 protein (supplementary material Fig. S1B) (Del Nagro et al., 2014; Mirzayans et al., 2013; Radha et al., 1999; Wrede et al., 1991). Our experiments (described above) established that BrdU-mediated direct DNA damage induces senescence in both HeLa and A549 cells, meaning that p53 is dispensable for induction of cellular senescence. This was confirmed using another agent genotoxic agent Dox, which also induced cellular senescence as described above. Interestingly, the ROS induction was higher in p53-positive A549 cells than in HeLa cells, as p53 positively regulates ROS to reinforce the DDR (Liu et al., 2008) (Fig. 1B).

To further evaluate the importance of p53 protein in senescence, the p53 expression in A549 cells was knocked down using specific shRNA. As shown in the supplementary material Fig. S4D, the expression of p53 was drastically reduced in the knockdown cells and we found that the basal ROS levels



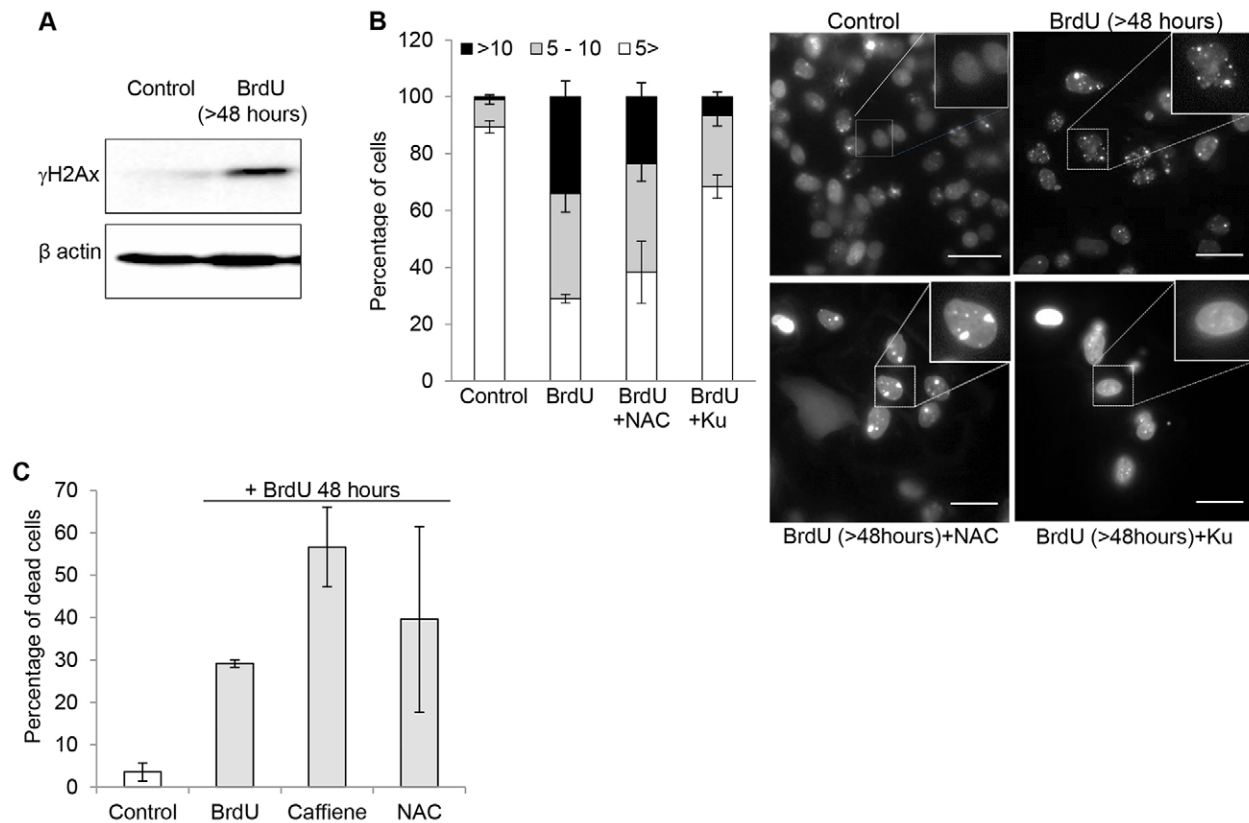


**Fig. 6. Effect of ROS quenching and ATM inhibition on maintenance of cellular senescence.** For all experiments HeLa cells were treated with BrdU for more than 48 h along with the inhibitors indicated. (A)  $\gamma$ H2AX analysis. Protein lysate from treated HeLa cells was used for western blotting and probed with anti-phospho-H2AX antibody as described Fig. 1A. A representative blot from two experiments is shown. (B) 53BP1 foci formation analysis. HeLa cells stably expressing 53BP1-GFP protein was treated with BrdU for more than 48 h followed by treatment with 5 mM NAC or 10  $\mu$ M Ku55933 (Ku) for more than 24 h and then imaged. The percentage of foci formed per cell was assessed as described in Fig. 2B. (C) Dead cell quantification. HeLa cells were treated with 100  $\mu$ M BrdU and after 48–72 h of treatment, cells were treated with 5 mM NAC or 2 mM caffeine. After 48 h the cell number was quantified as described in Fig. 2D. Scale bars: 40  $\mu$ m. Results are mean  $\pm$  s.e.m.

were significantly higher (supplementary material Fig. S4D), suggesting that the inactive p53 acts as a negative regulator of ROS, similar to what has been observed previously (Sablina et al., 2005). When these cells were treated with BrdU or Dox to induce senescence, we observed that cells underwent senescence as anticipated, but the fold increase in ROS after treatment was significantly lower in comparison to wild-type cells (supplementary material Fig. S4E). These results strengthened our observations that p53 is dispensable in senescence and basically serves as an amplifier of the DDR by regulating the production of ROS in cells.

## DISCUSSION

Cellular senescence is a state where cells permanently stop dividing in response to genomic instability. It can be induced even in immortal and cancer cells, which have overcome the replicative exhaustion or oncogene activation barrier, by exposing them to a sub-lethal dose of genotoxic stress, making this process a very attractive tumor-suppressing process. Current cellular senescence models enlist ATM protein as one of the central nodes in the senescence cascade (Colavitti and Finkel, 2005; d'Adda di Fagagna, 2008; von Zglinicki et al., 2005), which is tightly linked to ROS levels (Liu et al., 2008; Shiloh and Ziv, 2013). Although it has not been proven conclusively, it has been suggested that ATM kinase is one of the key proteins in the cell fate decision

process that is activated by the DNA DSBs (Lee and Paull, 2005), and that it could be the sensor responsible for quantifying DNA damage (Guo et al., 2010). Under conditions where DNA damage is not severe, DNA repair takes place, which allows growth, and when the damage is severe, a cellular apoptosis program is initiated (d'Adda di Fagagna, 2008). In cases where the damage is of intermediate nature, ATM kinase leads to activation of cellular senescence wherein cells are trapped in a viable but non-proliferating state (Shiloh and Ziv, 2013; von Zglinicki et al., 2005). In our studies to evaluate the regulatory role of ATM kinase and ROS in cellular senescence, we utilized direct DNA damage to initiate the DDR, which allowed us to bypass stress-mediated effects produced by other agents such as ionizing radiation, Dox and peroxide. Using direct DNA damage treatment, we determined that the amount of ATM kinase activation correlated with the amount of DNA damage present in the cell (i.e. the dose of BrdU).

As mentioned above, existing models of cellular senescence implicate ATM kinase, ROS and p53 as key regulatory molecules. For p53 protein, many reports have proposed diametrically opposite roles in regulating cellular senescence; some studies propose that sustained p53 activation is responsible for senescence initiation and maintenance (Purvis et al., 2012; Rufini et al., 2013), whereas several other studies show that p53 is dispensable and senescence can be governed by p21 or p16 (also

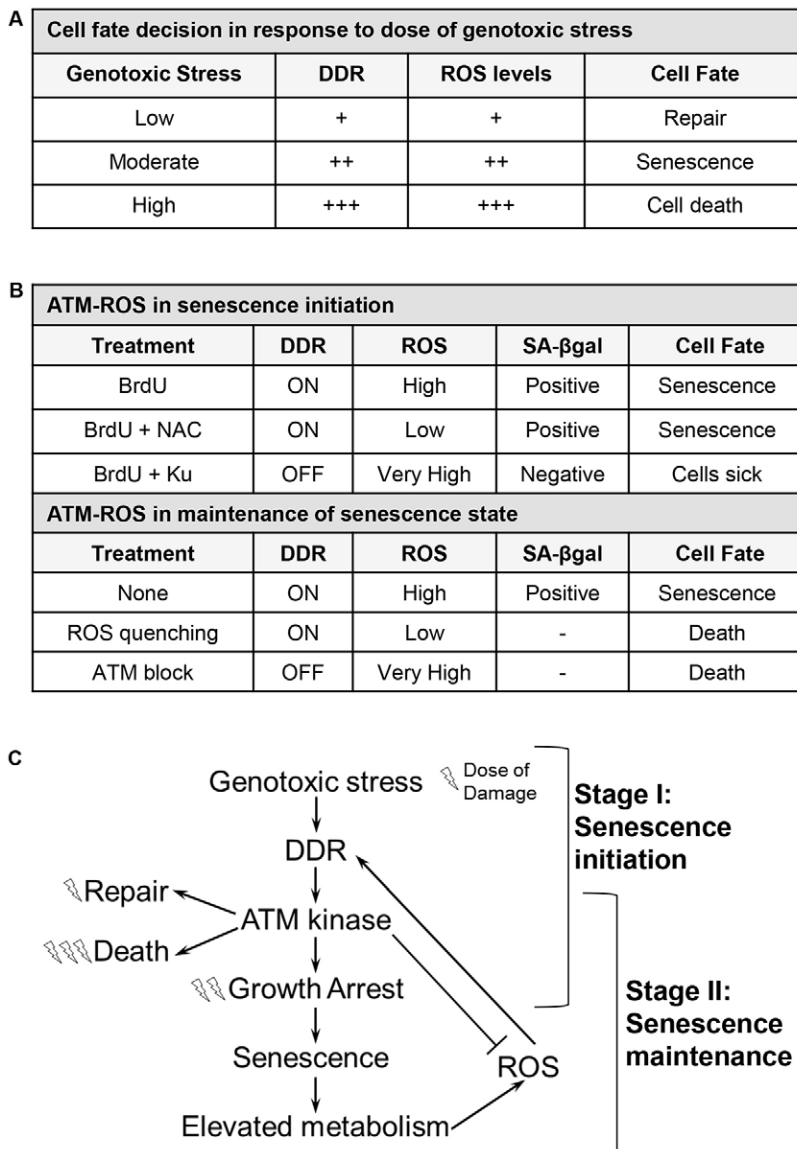


**Fig. 7. Cell fate decision and cellular senescence.** (A) The dose of the DNA-damaging agent is linked to cell fate. Table summarizing the effect of amount of DNA damage on cell fate and other components. (B) ATM kinase and ROS in cellular senescence. Table summarizing the role played by the ATM kinase and ROS in the two stages of cellular senescence. (C) Model depicting the regulation of two stages of cellular senescence: (I) ATM kinase activity is proportional to the amount of genotoxic stress and (II) ATM kinase plays a role in both stages, whereas ROS are only essential in the maintenance stage of cellular senescence.

known as CDKN2A) proteins alone (Aliouat-Denis et al., 2005; Ben-Porath and Weinberg, 2005). Similar to p53, ROS has also been projected as a crucial molecule that regulates and maintains senescence, as it can damage DNA, proteins and lipids to induce the stress response, which in turn can affect the senescence phenotype (Colavitti and Finkel, 2005; Lu and Finkel, 2008; Macip et al., 2002). Given that most of the chemically induced senescence protocols use agents like ionizing radiation and peroxide, which generate ROS, to induce senescence, the role of ROS in DNA damage has been found to be absolutely crucial.

We found that cells exposed to the direct DNA-damage-inducing agent BrdU induced standard senescence markers, such as p21, fibronectin, IL8 and others, as reported previously (Masterson and O'Dea, 2007; Eriko et al., 1999; Suzuki et al., 2001), and that they are positive for SA- $\beta$ -gal and show enhanced secretion of IL8 (Cho et al., 2011), which is similar to what is observed in senescent cells generated by other approaches (Coppé et al., 2008). We utilized this unique direct DNA damage approach to activate senescence in cancer cells to determine whether ATM kinase and ROS play distinct roles in the initiation

and maintenance of senescence. ROS was found to be crucial only in the maintenance stage, whereas the activation of ATM kinase was essential in both initiation and maintenance stages of senescence. These findings allow us to propose distinct regulatory events for both the stages of cellular senescence. The first stage is initiated after detection of the amount of DNA damage through activation of ATM kinase and does not require ROS. The second stage involves maintenance of senescent state of cells through both ROS and ATM kinase (Ditch and Paull, 2012; Guo et al., 2010; Shiloh and Ziv, 2013) (Fig. 7). This and other previous studies propose that activation of ATM kinase occurs through ROS, and suggest that ATM kinase is responsible for protecting the cells from the harmful effects of ROS through activation of enzymes such as superoxide dismutases and catalases. Hence, ROS levels are significantly higher in cells where ATM is inhibited (Shiloh and Ziv, 2013). The elevated ROS levels in senescent cells causes DSBs and keeps ATM kinase in activated state (Lee and Paull, 2004; Lee and Paull, 2005), thereby keeping cells in a growth-arrested state. This is crucial given that cells that have been exposed to high doses of genotoxic stress might

become cancerous if left unchecked, even if DNA damage is repaired. Concomitant with this, the deactivation of ATM in senescent cells leads to accumulation of ROS, which triggers cell death.

Aging and the cellular senescence process have always been associated with oxidative damage due to accumulation of ROS (Chen and Ames, 1994; Colavitti and Finkel, 2005). Studies also show that ROS cause oxidative damage to many cellular components, such as DNA, proteins and lipids, which in turn induce cellular senescence. The senescence model used here shows that senescence-associated markers are present even when the ROS had been quenched in the cells during the initiation phase. We suggest that direct DNA damage and the DDR alone can induce senescence, independently of ROS-mediated secondary responses, and that this is also not dependent on the p53 status of the cells. Furthermore, based on the work described here and other previous reports, it is also possible to speculate that although p53 is induced during the DDR, it is not the cause, but the effect of the DDR, similar to ROS. This further strengthens the idea of utilizing cellular senescence as an approach to regulate cancer cell proliferation, even in tumors which are deficient in p53 protein. We show that p53 protein essentially acts as a DDR amplifier in senescence, wherein induction of p53 in response to DDR causes enhancement of ROS levels. Such an impact of activated p53 is known in literature, where activated p53 protein increases the ROS levels through direct activation of enzymes such as proline oxidase (POX) and quinone oxidoreductase (NOQ1), which generate ROS (Polyak et al., 1997).

In summary, we demonstrate that ROS and p53, which are considered to be crucial mediators of cellular senescence, are not really essential for the initiation of the senescence program. Activation of ATM kinase either through direct DNA damage or any other mode is sufficient to initiate senescence. This is different in the maintenance stage of senescence, where both ROS and ATM kinase are crucial. Overall, we find that ATM kinase plays a central role in cellular senescence, ROS are crucial only in the maintenance of cellular senescence and that p53 protein acts as an amplifier and strengthens the senescent phenotype.

## MATERIALS AND METHODS

All chemicals were from Sigma Aldrich, USA and antibodies from Cell Signaling Technology, USA unless otherwise stated.

### Cell culture

HeLa and A549 cells (ATCC, USA) were grown overnight at 37°C; 5% CO<sub>2</sub> and were treated with various DNA-damaging agents as described below. For expression knockdown, validated shRNA for ATM kinase and p53 genes from TRC library were used. ATM shRNA was transfected in HeLa cells and p53 shRNA were introduced in A549 cells by lentiviral transduction (Davidson and Harper, 2005) and stable knockdown cells were selected on puromycin (3 µg/ml) for 48 h. The knockdown efficiency was verified in the stable cells by semi-quantitative RT-PCR analysis or by western blotting as described below.

To induce DNA damage, the cells were treated with 5-bromodeoxyuridine (prepared fresh in DMSO) or doxorubicin (1 mg/ml in water) for the indicated time durations. For ionizing-radiation-induced damage, cells were treated with 1 Gy units of  $\gamma$ -radiation (Blood irradiator BI 2000) and allowed to adhere overnight before further analysis. The treated and untreated cells were processed for various experimental analyses as described below.

### ROS analysis

For ROS detection, cells were incubated with 10 µM 2',7'-dichlorofluorescein (DCFDA) in 1× PBS for 30 min in dark. Cells are

washed with PBS three times and analyzed to detect DCF fluorescence (Infinite F200, Tecan, Austria). The excitation wavelength was 492 nm and the emission wavelength was 525 nm. For ROS quenching, 5 mM N-acetyl L-cysteine (NAC) was used and along with 100 µM BrdU for 48 h in senescence experiments. For few experiments, cells were counted and DCFDA fluorescence was determined as fluorescence per cell and for few experiments, along the DCFDA, DAPI was added (excitation, 345 nm; emission, 455 nm), the fluorescence from DCFDA was normalized to that of DAPI.

### 53BP1 foci formation assay

To generate 53BP1 sensor for DNA damage response, the minimal region of 492 amino acids (from position 1220 to 1711) of 53BP1 protein sufficient for foci formation during the DDR (Zgheib et al., 2009) was amplified from cDNA from HeLa cells and cloned into pEGFP-C1 vector at the *KpnI* and *XhoI* sites. The recombinant GFP-53BP1-encoding vector was transfected into HeLa cells and positive cells were sorted using a BD-FACS Aria cell sorter (BD Biosciences, USA). The GFP-53BP1-positive HeLa cells were propagated by culturing with G418. For imaging, the cells were seeded on glass-bottomed dishes (NEST, China), treated as indicated and then imaged using a fluorescence inverted epifluorescence microscope (Olympus IX83, Japan). The excitation wavelength was selected by using a Spectra X light engine (Lumencor Inc., USA) and band pass filters in a high speed filter wheel (ASI Inc., USA) were used for detection of the emission wavelength. The images were acquired using Evolve 512 EMCCD camera (Photometrics, USA), under controlled conditions using a Uno CO<sub>2</sub> incubation system (OKOLab, Italy). All devices were controlled using Slidebook 6 software (3i Inc., USA). For quantification, the number of foci present in each cell was manually counted for a minimum of 100 cells per dish. For representation, the brightness and contrast of the images were adjusted with the Microsoft Office Image editing tool.

### Cell cycle profiling

The cell cycle was profiled with propidium iodide using standard protocols. Cells were trypsinized and fixed with 70% cold ethanol and stored overnight at -20°C. The fixed cells were pelleted, washed and incubated overnight in 1× PBS with 0.15 mg/ml RNase A (Amresco, USA) at 37°C. Cells were then incubated for 10 min with 50 µg/ml propidium iodide in dark. Subsequent cell cycle analysis was performed in a FACS Calibur (BD Biosciences, USA) flow cytometer, using a 15 mW 488 nm laser, and data was analyzed using CellQuest Pro Software.

### Gene expression profiling

Total RNA from cell lines was isolated by using the TRI reagent and cDNA synthesis was performed using the Invitrogen Superscript III First Strand Synthesis System (Thermo Scientific Inc., USA) as per the manufacturer's instructions. Gene-specific quantitative real-time PCR analysis was performed using an ABI 7500 cycler (Thermo Scientific Inc., USA) using a DyNamo Color Flash SYBR Green qPCR Kit (Thermo Scientific, USA) in 20 µl reaction volume according to the manufacturer's instructions. Expression levels of  $\beta$ -actin and GAPDH were used for normalization. ABI systems SDS 2.3 software was used for data analysis. Primers used for analysis are described in supplementary material Table S1.

### Rezasurin assay for estimation of cellular metabolic activity

Equal number of senescent cells (BrdU treated for 48 h) and control cells were seeded in a 96-well black PS plate (SPL Plastics, Korea) and were maintained overnight in serum-free Dulbecco's modified Eagle's medium (DMEM). Rezasurin dye was added to wells at a final concentration of 10 µg/ml and incubated for 3–5 h in 5% CO<sub>2</sub>, 37°C incubator. After the incubation the plate was recorded for fluorescence (excitation 560 nm; emission and 590 nm) using a multiwell plate reader (Infinite F200, Tecan, Austria).

### Western blot analysis

Cell lysate was prepared using ProteoJET Mammalian Cell Lysis Reagent (Fermentas Inc., USA) according to the manufacturer's

protocol and the amount of total protein was estimated using Bradford's reagent. For analysis, 50 µg of total protein was resolved on a 12.5% SDS-PAGE gel, transferred onto PVDF membrane (GE Healthcare, USA) using a semi-dry transfer unit (GE Healthcare, USA) at 60 mA for 60 min. The membrane-containing transferred protein was blocked with 5% non-fat milk protein in Tris-buffered saline with Tween 20 (TBST) for 1 h. The membrane was probed overnight with primary antibody at 4°C. Membranes were washed three times for 10 min in TBST and incubated with the appropriate horseradish peroxidase (HRP)-tagged secondary antibodies (Jackson Laboratories Inc., USA) diluted at manufacturer's recommendations at room temperature for 1 h. Membranes were again washed three times with TBST and subjected to chemiluminescent detection using ECL substrate (Western Lightning Plus, PerkinElmer, USA). The developed blots were imaged and analyzed using the ChemiDoc MP Imaging system (Bio-Rad Inc., USA). β-actin expression was used as a loading control.

### SA-β-gal staining for senescent cells

The protocol described by Dimri et al. was followed for SA-β-gal staining (Dimri et al., 1995). Cells were washed in PBS, fixed for 15 min at room temperature in 0.2% glutaraldehyde (Amresco, USA) in 1× PBS, washed three times with PBS and incubated overnight at 37°C (without CO<sub>2</sub>) with freshly prepared staining solution (1 mg/ml X-gal; GoldBio Technology, USA) in 40 mM citric acid/sodium phosphate, pH 6.0, 5 mM potassium ferrocyanide, 5 mM potassium ferricyanide, 150 mM NaCl and 2 mM MgCl<sub>2</sub> (all chemicals from SRL, India). After overnight incubation, the cells were washed with 1× PBS and imaged for presence of blue color in the cells. The imaging was done using an inverted IX81 microscope, equipped with a DP72 color camera (Olympus, Japan).

### IL6 and IL8 quantification

The amounts of IL6 and IL8 cytokines were quantified using 100 µl of medium collected from cells using the Human IL6 high sensitivity ELISA kit (eBioscience Inc., USA) and BD OptiEIA™ Human IL8 ELISA kit (BD Biosciences, USA) according to the manufacturer's instructions. The cells were counted from the same wells to normalize the amount to the number of cells (amount per 10<sup>3</sup> cells).

### Analysis of phosphorylated ATM levels

Treated cells were fixed with 4% paraformaldehyde for 15 min, washed three times with 1× PBS for 5 min and were then permeabilized using 1% Triton X-100 for 15 min and blocked using 0.5% BSA for 45 min. After blocking, cells were probed overnight with anti-phosphorylated-ATM antibody (1:100 dilution) at 4°C. The cells were washed three times with 1× PBS for 10 min each and incubated with secondary antibody conjugated to Alexa Fluor 488 (Invitrogen Molecular Probes) for 45 min at room temperature in the dark. After washing with 1× PBS, coverslips were mounted onto glass slides with DAPI and sealed before imaging. The images were collected using IX83 inverted fluorescence microscope at various z-planes, deconvolved using a nearest neighbor algorithm and a maximum intensity projection was generated using Slidebook 6 software (3i, USA).

### Acknowledgements

Prof. Dipankar Nandi and Prof. Sandhya Visweswariah, IISc are acknowledged for their valuable suggestions.

### Competing interests

The authors declare no competing or financial interests.

### Author contributions

R.R.N. designed and performed the experiments, analyzed the data and wrote the paper; M.B. contributed reagents and performed experiments; and D.K.S. designed the experiments, analyzed the data and wrote the paper.

### Funding

The study was supported by financial assistance from Department of Biotechnology, India (DBT) to D.K.S.; and through the DBT partnership program to the Indian Institute of Science. Equipment support provided by DST-FIST

program; and a Research Fellowship to R.R.N. from Council of Scientific & Industrial Research (CSIR) is acknowledged.

### Supplementary material

Supplementary material available online at <http://jcs.biologists.org/lookup/suppl/doi:10.1242/jcs.159517/-DC1>

### References

- Aliouat-Denis, C. M., Dendouga, N., Van den Wyngaert, I., Goehmann, H., Steller, U., van de Weyer, I., Van Slycken, N., Andries, L., Kass, S., Luyten, W. et al. (2005). p53-independent regulation of p21Waf1/Cip1 expression and senescence by Chk2. *Mol. Cancer Res.* **3**, 627–634.
- Aruoma, O. I., Halliwell, B., Hoey, B. M. and Butler, J. (1989). The antioxidant action of N-acetylcysteine: its reaction with hydrogen peroxide, hydroxyl radical, superoxide, and hypochlorous acid. *Free Radic. Biol. Med.* **6**, 593–597.
- Barascu, A., Le Chalony, C., Pennarun, G., Genet, D., Imam, N., Lopez, B. and Bertrand, P. (2012). Oxidative stress induces an ATM-independent senescence pathway through p38 MAPK-mediated lamin B1 accumulation. *EMBO J.* **31**, 1080–1094.
- Ben-Porath, I. and Weinberg, R. A. (2005). The signals and pathways activating cellular senescence. *Int. J. Biochem. Cell Biol.* **37**, 961–976.
- Blasina, A., Price, B. D., Turenne, G. A. and McGowan, C. H. (1999). Caffeine inhibits the checkpoint kinase ATM. *Curr. Biol.* **9**, 1135–1138.
- Chen, Q. and Ames, B. N. (1994). Senescence-like growth arrest induced by hydrogen peroxide in human diploid fibroblast F65 cells. *Proc. Natl. Acad. Sci. USA* **91**, 4130–4134.
- Chen, Q. M., Tu, V. C. and Liu, J. (2000). Measurements of hydrogen peroxide induced premature senescence: senescence-associated beta-galactosidase and DNA synthesis index in human diploid fibroblasts with down-regulated p53 or Rb. *Biogerontology* **1**, 335–339.
- Chen, J. H., Hales, C. N. and Ozanne, S. E. (2007). DNA damage, cellular senescence and organismal ageing: causal or correlative? *Nucleic Acids Res.* **35**, 7417–7428.
- Cho, J. H., Saini, D. K., Karunarathne, W. K., Kalyanaraman, V. and Gautam, N. (2011). Alteration of Golgi structure in senescent cells and its regulation by a G protein γ subunit. *Cell. Signal.* **23**, 785–793.
- Colavitti, R. and Finkel, T. (2005). Reactive oxygen species as mediators of cellular senescence. *IUBMB Life* **57**, 277–281.
- Cooke, M. S., Evans, M. D., Dizdaroglu, M. and Lunec, J. (2003). Oxidative DNA damage: mechanisms, mutation, and disease. *FASEB J.* **17**, 1195–1214.
- Coppé, J. P., Patil, C. K., Rodier, F., Sun, Y., Muñoz, D. P., Goldstein, J., Nelson, P. S., Desprez, P. Y. and Campisi, J. (2008). Senescence-associated secretory phenotypes reveal cell-nonautonomous functions of oncogenic RAS and the p53 tumor suppressor. *PLoS Biol.* **6**, e301.
- Coppé, J. P., Desprez, P. Y., Krtochka, A. and Campisi, J. (2010). The senescence-associated secretory phenotype: the dark side of tumor suppression. *Annu. Rev. Pathol.* **5**, 99–118.
- d'Adda di Fagnana, F. (2008). Living on a break: cellular senescence as a DNA-damage response. *Nat. Rev. Cancer* **8**, 512–522.
- Davidson, B. L. and Harper, S. Q. (2005). Viral delivery of recombinant short hairpin RNAs. *Methods Enzymol.* **392**, 145–173.
- Del Nagro, C. J., Choi, J., Xiao, Y., Rangell, L., Mohan, S., Pandita, A., Zha, J., Jackson, P. K. and O'Brien, T. (2014). Chk1 inhibition in p53-deficient cell lines drives rapid chromosome fragmentation followed by caspase-independent cell death. *Cell Cycle* **13**, 303–314.
- Di Micco, R., Fumagalli, M., Cicalese, A., Piccinin, S., Gasparini, P., Luise, C., Schurra, C., Garre, M., Nuciforo, P. G., Bersimon, A. et al. (2006). Oncogene-induced senescence is a DNA damage response triggered by DNA hyper-replication. *Nature* **444**, 638–642.
- Dimri, G. P., Lee, X., Basile, G., Acosta, M., Scott, G., Roskelley, C., Medrano, E. E., Linskens, M., Rubelj, I., Pereira-Smith, O. et al. (1995). A biomarker that identifies senescent human cells in culture and in aging skin in vivo. *Proc. Natl. Acad. Sci. USA* **92**, 9363–9367.
- Ditch, S. and Paull, T. T. (2012). The ATM protein kinase and cellular redox signaling: beyond the DNA damage response. *Trends Biochem. Sci.* **37**, 15–22.
- Duan, J., Duan, J., Zhang, Z. and Tong, T. (2005). Irreversible cellular senescence induced by prolonged exposure to H<sub>2</sub>O<sub>2</sub> involves DNA-damage-and-repair genes and telomere shortening. *Int. J. Biochem. Cell Biol.* **37**, 1407–1420.
- Dumont, P., Burton, M., Chen, Q. M., Gonos, E. S., Fripiat, C., Mazarati, J. B., Eliaers, F., Remacle, J. and Toussaint, O. (2000). Induction of replicative senescence biomarkers by sublethal oxidative stresses in normal human fibroblast. *Free Radic. Biol. Med.* **28**, 361–373.
- Eriko, M., Nakabayashi, K., Suzuki, T., Kaul, S. C., Ogino, H., Fujii, M., Mitsui, Y. and Ayusawa, D. (1999). 5-Bromodeoxyuridine induces senescence-like phenomena in mammalian cells regardless of cell type or species. *J. Biochem.* **126**, 1052–1059.
- Erol, A. (2011). Genotoxic stress-mediated cell cycle activities for the decision of cellular fate. *Cell Cycle* **10**, 3239–3248.
- Freund, A., Orjalo, A. V., Desprez, P. Y. and Campisi, J. (2010). Inflammatory networks during cellular senescence: causes and consequences. *Trends Mol. Med.* **16**, 238–246.

- Furumoto, K., Inoue, E., Nagao, N., Hiyama, E. and Miwa, N. (1998). Age-dependent telomere shortening is slowed down by enrichment of intracellular vitamin C via suppression of oxidative stress. *Life Sci.* **63**, 935–948.
- Gewirtz, D. A. (1999). A critical evaluation of the mechanisms of action proposed for the antitumor effects of the anthracycline antibiotics adriamycin and daunorubicin. *Biochem. Pharmacol.* **57**, 727–741.
- Guo, Z., Kozlov, S., Lavin, M. F., Person, M. D. and Paull, T. T. (2010). ATM activation by oxidative stress. *Science* **330**, 517–521.
- Hayflick, L. (1965). The limited in vitro lifetime of human diploid cell strains. *Exp. Cell Res.* **37**, 614–636.
- Hickson, I., Zhao, Y., Richardson, C. J., Green, S. J., Martin, N. M., Orr, A. I., Reaper, P. M., Jackson, S. P., Curtin, N. J. and Smith, G. C. (2004). Identification and characterization of a novel and specific inhibitor of the ataxia-telangiectasia mutated kinase ATM. *Cancer Res.* **64**, 9152–9159.
- Itahana, K., Campisi, J. and Dimri, G. P. (2007). Methods to detect biomarkers of cellular senescence: the senescence-associated beta-galactosidase assay. *Methods Mol. Biol.* **371**, 21–31.
- Ivanov, V. N., Zhou, H., Partridge, M. A. and Hei, T. K. (2009). Inhibition of ataxia telangiectasia mutated kinase activity enhances TRAIL-mediated apoptosis in human melanoma cells. *Cancer Res.* **69**, 3510–3519.
- Jeyapalan, J. C. and Sedivy, J. M. (2008). Cellular senescence and organismal aging. *Mech. Ageing Dev.* **129**, 467–474.
- Kanaar, R., Hoeijmakers, J. H. and van Gent, D. C. (1998). Molecular mechanisms of DNA double strand break repair. *Trends Cell Biol.* **8**, 483–489.
- Kang, M. A., So, E. Y., Simons, A. L., Spitz, D. R. and Ouchi, T. (2012). DNA damage induces reactive oxygen species generation through the H2AX-Nox1/Rac1 pathway. *Cell Death Dis.* **3**, e249.
- Krtolica, A., Parrinello, S., Lockett, S., Desprez, P. Y. and Campisi, J. (2001). Senescent fibroblasts promote epithelial cell growth and tumorigenesis: a link between cancer and aging. *Proc. Natl. Acad. Sci. USA* **98**, 12072–12077.
- Kuilman, T., Michaloglou, C., Mooi, W. J. and Peeeper, D. S. (2010). The essence of senescence. *Genes Dev.* **24**, 2463–2479.
- Kumazaki, T., Robetorye, R. S., Robetorye, S. C. and Smith, J. R. (1991). Fibronectin expression increases during in vitro cellular senescence: correlation with increased cell area. *Exp. Cell Res.* **195**, 13–19.
- Lawless, C., Wang, C., Jurk, D., Merz, A., Zglinicki, T. and Passos, J. F. (2010). Quantitative assessment of markers for cell senescence. *Exp. Gerontol.* **45**, 772–778.
- Lee, J. H. and Paull, T. T. (2004). Direct activation of the ATM protein kinase by the Mre11/Rad50/Nbs1 complex. *Science* **304**, 93–96.
- Lee, J. H. and Paull, T. T. (2005). ATM activation by DNA double-strand breaks through the Mre11-Rad50-Nbs1 complex. *Science* **308**, 551–554.
- Lee, A. C., Fenster, B. E., Ito, H., Takeda, K., Bae, N. S., Hirai, T., Yu, Z. X., Ferrans, V. J., Howard, B. H. and Finkel, T. (1999). Ras proteins induce senescence by altering the intracellular levels of reactive oxygen species. *J. Biol. Chem.* **274**, 7936–7940.
- Leontieva, O. V. and Blagosklonny, M. V. (2010). DNA damaging agents and p53 do not cause senescence in quiescent cells, while consecutive re-activation of mTOR is associated with conversion to senescence. *Ageing (Albany, NY)* **2**, 924–935.
- Li, Y. and Yang, D. Q. (2010). The ATM inhibitor KU-55933 suppresses cell proliferation and induces apoptosis by blocking Akt in cancer cells with overactivated Akt. *Mol. Cancer Ther.* **9**, 113–125.
- Liu, B., Chen, Y. and St Clair, D. K. (2008). ROS and p53: a versatile partnership. *Free Radic. Biol. Med.* **44**, 1529–1535.
- Lu, T. and Finkel, T. (2008). Free radicals and senescence. *Exp. Cell Res.* **314**, 1918–1922.
- Macip, S., Igarashi, M., Fang, L., Chen, A., Pan, Z. Q., Lee, S. W. and Aaronson, S. A. (2002). Inhibition of p21-mediated ROS accumulation can rescue p21-induced senescence. *EMBO J.* **21**, 2180–2188.
- Maicher, A., Kastner, L., Dees, M. and Luke, B. (2012). Deregulated telomere transcription causes replication-dependent telomere shortening and promotes cellular senescence. *Nucleic Acids Res.* **40**, 6649–6659.
- Mao, Z., Ke, Z., Gorbunova, V. and Seluanov, A. (2012). Replicatively senescent cells are arrested in G1 and G2 phases. *Ageing (Albany, NY)* **4**, 431–435.
- Masterson, J. C. and O’Dea, S. (2007). 5-Bromo-2-deoxyuridine activates DNA damage signalling responses and induces a senescence-like phenotype in p16-null lung cancer cells. *Anticancer Drugs* **18**, 1053–1068.
- Matlashewski, G., Banks, L., Pim, D. and Crawford, L. (1986). Analysis of human p53 proteins and mRNA levels in normal and transformed cells. *Eur. J. Biochem.* **154**, 665–672.
- Mirzayans, R., Andrais, B., Scott, A., Wang, Y. W. and Murray, D. (2013). Ionizing radiation-induced responses in human cells with differing TP53 status. *Int. J. Mol. Sci.* **14**, 22409–22435.
- Mishra, K. P. (2004). Cell membrane oxidative damage induced by gamma-radiation and apoptotic sensitivity. *J. Environ. Pathol. Toxicol. Oncol.* **23**, 61–66.
- Mizutani, H., Tada-Oikawa, S., Hiraku, Y., Kojima, M. and Kawanishi, S. (2005). Mechanism of apoptosis induced by doxorubicin through the generation of hydrogen peroxide. *Life Sci.* **76**, 1439–1453.
- Mukhopadhyay, P., Rajesh, M., Bátkai, S., Kashiwaya, Y., Haskó, G., Liaudet, L., Szabó, C. and Pachter, P. (2009). Role of superoxide, nitric oxide, and peroxynitrite in doxorubicin-induced cell death in vivo and in vitro. *Am. J. Physiol.* **296**, H1466–H1483.
- Passos, J. F. and Von Zglinicki, T. (2006). Oxygen free radicals in cell senescence: are they signal transducers? *Free Radic. Res.* **40**, 1277–1283.
- Passos, J. F., Simillion, C., Hallinan, J., Wipat, A. and von Zglinicki, T. (2009). Cellular senescence: unravelling complexity. *Age (Dordr.)* **31**, 353–363.
- Polyak, K., Xia, Y., Zweier, J. L., Kinzler, K. W. and Vogelstein, B. (1997). A model for p53-induced apoptosis. *Nature* **389**, 300–305.
- Pospelova, T. V., Demidenko, Z. N., Bukreeva, E. I., Pospelov, V. A., Gudkov, A. V. and Blagosklonny, M. V. (2009). Pseudo-DNA damage response in senescent cells. *Cell Cycle* **8**, 4112–4118.
- Purvis, J. E., Karhohs, K. W., Mock, C., Batchelor, E., Loewer, A. and Lahav, G. (2012). p53 dynamics control cell fate. *Science* **336**, 1440–1444.
- Qu, K., Lin, T., Wang, Z., Liu, S., Chang, H., Xu, X., Meng, F., Zhou, L., Wei, J., Tai, M. et al. (2014). Reactive oxygen species generation is essential for cisplatin-induced accelerated senescence in hepatocellular carcinoma. *Front Med.* **8**, 227–235.
- Radha, V., Sudhakar, C. and Swarup, G. (1999). Induction of p53 dependent apoptosis upon overexpression of a nuclear protein tyrosine phosphatase. *FEBS Lett.* **453**, 308–312.
- Rodier, F., Coppé, J. P., Patil, C. K., Hoeijmakers, W. A., Muñoz, D. P., Raza, S. R., Freund, A., Campeau, E., Davalos, A. R. and Campisi, J. (2009). Persistent DNA damage signalling triggers senescence-associated inflammatory cytokine secretion. *Nat. Cell Biol.* **11**, 973–979.
- Roninson, I. B. (2002). Oncogenic functions of tumour suppressor p21(Waf1/Cip1/Sd1): association with cell senescence and tumour-promoting activities of stromal fibroblasts. *Cancer Lett.* **179**, 1–14.
- Rufini, A., Tucci, P., Celardo, I. and Melino, G. (2013). Senescence and aging: the critical roles of p53. *Oncogene* **32**, 5129–5143.
- Sablina, A. A., Budanov, A. V., Ilyinskaya, G. V., Agapova, L. S., Kravchenko, J. E. and Chumakov, P. M. (2005). The antioxidant function of the p53 tumor suppressor. *Nat. Med.* **11**, 1306–1313.
- Schneider, E. L. and Mitsui, Y. (1976). The relationship between in vitro cellular aging and in vivo human age. *Proc. Natl. Acad. Sci. USA* **73**, 3584–3588.
- Serrano, M., Lin, A. W., McCurrach, M. E., Beach, D. and Lowe, S. W. (1997). Oncogenic ras provokes premature cell senescence associated with accumulation of p53 and p16INK4a. *Cell* **88**, 593–602.
- Shiloh, Y. and Ziv, Y. (2013). The ATM protein kinase: regulating the cellular response to genotoxic stress, and more. *Nat. Rev. Mol. Cell Biol.* **14**, 197–210.
- Sliwinski, M. A., Mosieniak, G., Wolanin, K., Babik, A., Piwocka, K., Magalska, A., Szczepanowska, J., Fronk, J. and Sikora, E. (2009). Induction of senescence with doxorubicin leads to increased genomic instability of HCT116 cells. *Mech. Ageing Dev.* **130**, 24–32.
- Surova, O. and Zhivotovsky, B. (2013). Various modes of cell death induced by DNA damage. *Oncogene* **32**, 3789–3797.
- Suzuki, T., Minagawa, S., Eriko, M., Ogino, H., Fujii, M., Mitsui, Y. and Ayusawa, D. (2001). Induction of senescence-associated genes by 5-bromodeoxyuridine in HeLa cells. *Exp. Gerontol.* **36**, 465–474.
- Tewey, K. M., Rowe, T. C., Yang, L., Halligan, B. D. and Liu, L. F. (1984). Adriamycin-induced DNA damage mediated by mammalian DNA topoisomerase II. *Science* **226**, 466–468.
- Thorn, C. F., Oshiro, C., Marsh, S., Hernandez-Boussard, T., McLeod, H., Klein, T. E. and Altman, R. B. (2011). Doxorubicin pathways: pharmacodynamics and adverse effects. *Pharmacogenet. Genomics* **21**, 440–446.
- van Maanen, J. M., Retèl, J., de Vries, J. and Pinedo, H. M. (1988). Mechanism of action of antitumor drug etoposide: a review. *J. Natl. Cancer Inst.* **80**, 1526–1533.
- von Zglinicki, T., Saretzki, G., Ladhoff, J., d’Adda di Fagagna, F. and Jackson, S. P. (2005). Human cell senescence as a DNA damage response. *Mech. Ageing Dev.* **126**, 111–117.
- Wrede, D., Tidy, J. A., Crook, T., Lane, D. and Vousden, K. H. (1991). Expression of RB and p53 proteins in HPV-positive and HPV-negative cervical carcinoma cell lines. *Mol. Carcinog.* **4**, 171–175.
- Yokochi, T. and Robertson, K. D. (2004). Doxorubicin inhibits DNMT1, resulting in conditional apoptosis. *Mol. Pharmacol.* **66**, 1415–1420.
- Zafarullah, M., Li, W. Q., Sylvester, J. and Ahmad, M. (2003). Molecular mechanisms of N-acetylcysteine actions. *Cell. Mol. Life Sci.* **60**, 6–20.
- Zgheib, O., Pataky, K., Brugger, J. and Halazonetis, T. D. (2009). An oligomerized 53BP1 tudor domain suffices for recognition of DNA double-strand breaks. *Mol. Cell Biol.* **29**, 1050–1058.